

## Observation of Interplanetary Scintillation with Single-Station Mode at Urumqi

Lijia Liu<sup>1</sup>, Xizhen Zhang<sup>1</sup>, Jianbin Li<sup>1</sup>, P.K. Manoharan<sup>2</sup>, Zhiyong Liu<sup>3</sup> and Bo Peng<sup>1</sup>

<sup>1</sup> National Astronomical Observatories, Chinese Academy of Sciences, Beijing 100012, China; [liulijiaredstar@yahoo.com.cn](mailto:liulijiaredstar@yahoo.com.cn), [lijb@bao.ac.cn](mailto:lijb@bao.ac.cn), [zxz@bao.ac.cn](mailto:zxz@bao.ac.cn), [pb@bao.ac.cn](mailto:pb@bao.ac.cn)

<sup>2</sup> Radio Astronomy Center, TIFR-NCRA, P.O. Box 8, Ooty 643 001, India; [mano@ncra.tifr.res.in](mailto:mano@ncra.tifr.res.in)

<sup>3</sup> Urumqi Observatory, NAOC No.150 South Science Road Urumqi, Xinjiang 830011, China; [liuzhy@uao.ac.cn](mailto:liuzhy@uao.ac.cn)

**Abstract** The Sun affects the Earth's physical phenomena in multiple ways, in particular the material in interplanetary space comes from coronal expansion in the form of inhomogeneous plasma flow (solar wind), which is the primary source of the interplanetary medium. Ground-based Interplanetary Scintillation (IPS) observations are an important and effective method for measuring solar wind speed and the structures of small diameter radio sources. We discuss one mode of ground-based single-station observations: Single-Station Single-Frequency (SSSF) mode. To realize the SSSF mode, a new system has been established at Urumqi Astronomical Observatory (UAO), China, and a series of experimental observations were carried out successfully from May to December, 2008.

**Key words:** IPS-SSSF-Observation

### 1 INTRODUCTION

Radiation from a distant compact radio source is scattered by the density irregularities in the solar wind plasma and produces a random diffraction pattern on the ground. The motion of these irregularities converts this pattern into temporal intensity fluctuations which are observed as interplanetary scintillation (IPS). IPS observations with ground-based telescopes can estimate the solar wind velocity and also the structures of the distant compact radio sources (Hewish & Symonds 1969; Armstrong & Coles 1972). This kind of measurement, though indirect, can give information on the solar wind out of the ecliptic plane and close to the Sun, where direct spacecraft measurements are not possible (e.g. Ma 1993). Here we concentrate on extracting information on solar wind speed from IPS observations with ground-based single telescope.

There are two modes to observe the IPS phenomenon with a single-station: Single-Station Single-Frequency (SSSF) and Single-Station Dual-Frequency (SSDF). Since the discovery of the IPS phenomenon (Hewish et.al. 1964), many countries began doing IPS observations with the single-station method, i.e. Cambridge telescope in Britain (Pruvis et al. 1987), Ooty radio telescope in India (Swarup et al. 1971), Puschino observatory in Russia (Vitkevich et al. 1976), one can use the power spectral fitting method to obtain the solar wind speed. With the multi-station method as used in Japan, which is a three-station system (Kojima et al. 1995), one can measure the projected solar wind speed directly. China began IPS studies from the 1990s with the phased array mode of the Miyun Synthesis Radio Telescope (MSRT) at 232 MHz. Located at Miyun observatory (Wang 1990) in Beijing, it used the SSSF mode (Wu & Zhang 2001). Recently a new IPS observation system using the 50 m parabolic radio telescope,

which is based on the SSDF mode at S/X and UHF bands, is under construction to serve the National Meridian Project of China.

In this paper, the theory of IPS, the technique, and the numerical simulation method of SSSF mode are introduced in section 2. The observations carried out at the UAO are reported in section 3. Finally conclusions are drawn in Section 4.

## 2 THEORY

### 2.1 The Theory of IPS

Interplanetary scintillation is the name given to the intensity fluctuations of small diameter radio sources which are caused by density inhomogeneities in the solar wind. Figure 1 shows the geometry of IPS. The distance between the Sun and  $Q$  is  $r$ , and  $r = \sin(\varepsilon)AU$ .

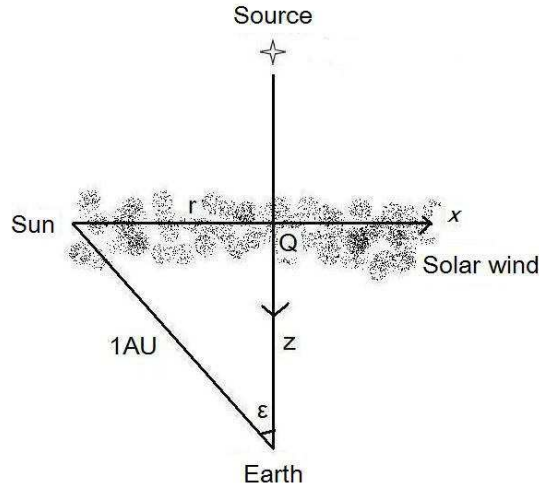


**Fig. 1** IPS Geometry:  $z$ -axis is along the line-of-sight,  $x$ -axis is in the direction perpendicular to the  $z$ -axis pointing away from the Sun, and  $y$ -axis is normal to the paper.  $Q$  is the point closest to the Sun along the line-of-sight, and  $\varepsilon$  is the elongation angle, Sun-Earth-source.  $r$  is the distance between the Sun and  $Q$ .  $Z$  is the distance between  $Q$  and the Earth.

The degree of scintillation is characterized by the scintillation index  $m$  (Cohen et al. 1967), which increases with decreasing distance  $r$  until it reaches a maximum  $m_{max}$  at  $r_{min}$ .  $r_{min}$  changes with frequency,  $r_{min} \approx 0.2AU$  for meter wavelength (Manoharan, 1993).

$$m = \frac{\sqrt{\sigma_{on}^2 - \sigma_{off}^2}}{C_{on} - C_{off}} \quad (1)$$

where  $C_{on}$  ( $C_{off}$ ) is the average intensity of the on-source (off-source) signal, and  $\sigma_{on}^2$  ( $\sigma_{off}^2$ ) is the square of rms of intensity scintillation. Here on-source case refers the telescope pointing at the radio source, and off-source the telescope pointing at the background sky away from the source, being in the opposite pitching direction to where the radio source moves. IPS is strongest in the region nearest the Sun, where we have the "strong scintillation region". In most of interplanetary space IPS is weak, which is called the "weak scintillation region" (Zhang 2006). In the weak scintillation region,  $m^2 \ll 1$ . The weak scintillation region is observed at  $r > r_{min}$  and strong scintillation is observed at  $r < r_{min}$ . Previous studies show that the statistics of the scintillation are simply related to those of the turbulent

interplanetary medium by a linear relationship, if the scintillation is weak (Coles & Harmon 1978). In the "strong scintillation region", however, the relationship is not straight forward, and the present study always deals with the weak scintillation case. The distance regime for the weak and strong regions relates to observing frequencies. Table 1 shows the relationship between the frequency and distance regimes (Zhang 2006).

Frequency (MHz)	150	327	900	2000	5000
Heliocentric distance (solar radius)	60	35	18	10	5

**Table 1** Regions of strong and weak scintillation at different frequencies. Taking 327 MHz for example, the regimes for the strong and weak regions are within 35 solar radius and beyond respectively.

In the weak scintillation region, where the radio wave can be treated as a plane-wave, and the Born approximation is applicable (e.g. Walker et al. 2004), the interplanetary medium can be considered to be made up of many thin layers perpendicular to the line-of-sight. When the radio wave passes through these layers, only the phase of the radio wave changes, while the amplitude of the radio wave stays the same. This is called the "thin screen approximation", which is commonly used in the study of the ionosphere, interplanetary medium, and interstellar medium.

## 2.2 SSSF Mode

SSSF refers to observing the IPS with a single station at a single frequency. There are two methods to obtain the solar wind speed from SSSF mode observed spectra: the spectral multi-parameter model-fitting, and the characteristic frequencies methods. The former can measure the speed by adjusting the main parameters of the solar wind to fit the observed scintillation power spectra. The parameters are:  $\alpha$ -power law index of the spatial spectrum of electron density, AR-axial ratio of solar wind irregularities, and  $V$ -solar wind speed. The latter can be determined by calculating two characteristic frequencies of the spectra: the Fresnel knee frequency  $f_F$ , and  $f_{min}$  the first minimum of the spectra. Then the solar wind speed can be calculated by either of the formulas shown below (Scott et al. 1983)

$$V = f_F \sqrt{Z\pi\lambda} \quad (2)$$

$$V = f_{min} \sqrt{Z\lambda} \quad (3)$$

where  $\lambda$  is the observing wavelength,  $Z$  is the distance between  $Q$  and the Earth as shown in Fig. 1. According to weak scintillation theory and thin screen approximation theory, in the weak scintillation region, the observed scintillation can be regarded as the sum of contributions from all the thin layers. For a layer of thickness  $dZ$ , the distance from the layer to the Earth is  $Z$ ,  $V_x(z)$  is the solar wind velocity projected on to the plane perpendicular to the direction  $z$ , and the spectra observed at the Earth should be (e.g. Scott et al. 1983; Ye & Qiu 1996):

$$M_s(f, Z)dZ = \frac{2\pi f(\lambda r_e)^2}{V_x(z)} \int_{-\infty}^{\infty} \Phi_{ne}(k_x, k_y, k_z = 0, Z) \times F_d F_s dk_y dZ \quad (4)$$

where,

$$F_d = 4 \sin^2 \left[ \frac{(k_x^2 + k_y^2) \lambda Z}{4\pi} \right] \quad (5)$$

$$F_s = \exp[-(k_x^2 + k_y^2) Z^2 \theta_0^2] \quad (6)$$

Here  $F_d$  and  $F_s$  are the Fresnel propagation filter parameter and the squared modulus of the radio source visibility. We assume that the brightness of the radio source has a symmetrical-Gaussian distribution, i.e.  $B(\theta) = \exp[\frac{-(\theta/\theta_0)^2}{2}]$ .  $\Theta$  is the full width at half maximum of the source, so we have the angular diameter of the scintillating source  $\theta_0 = \Theta/2.35$  (Manoharan & Ananthakrishnan 1990).  $\Phi_{ne}$  is the electron density power spectrum at distance  $z$ ,

$$\Phi_{ne}(k_x, k_y, k_z = 0, Z) = T r^{-4} [k_x^2 + (k_y/AR)^2]^{-\alpha/2} \quad (7)$$

where the amplitude of fluctuations in the electron density  $T$  is a constant. The spectrum obtained from the Earth should be the sum of Eq. (4).

$$M_i(f) = \int_0^\infty M_s(f, Z) dZ \quad (8)$$

One can see that  $M_i(f)$  depends on the solar wind parameters: axis ratio  $AR$ , power law index  $\alpha$ , and the solar wind speed  $V$ . Previous studies show that, when other parameters fixed,  $AR$  mostly affects the low frequency part of the power spectra; when  $AR$  increases, the low frequency part becomes steeper, but the high frequency part changes slightly.  $\alpha$  mostly affects the high frequency part of the spectra; when  $\alpha$  increases, the high frequency part attenuates quickly, but the low frequency part changes invidently. The solar wind speed  $V$  mostly affects the Fresnel knee  $f_F$  and the first minimum of the spectra  $f_{min}$ ; the two frequencies both become larger when  $V$  increases. Taking appropriate values to fit the observed spectra, one can obtain the parameters of the observational data. Firstly one fits the fresnel knee according to  $f_F$  and  $f_{min}$ , then fits the attenuated high part and the flat low frequency part. (Ye & Qiu 1996)

Fig.2 is an example of the SSSF mode. Where the parameters taken are  $\lambda = 92\text{cm}$ ,  $\alpha = 3.5$ ,  $AR = 2.0$ ,  $V = 600\text{km/s}$ ,  $\theta_0 = 0.02''$ . One can get  $f_F = 1.05\text{Hz}$ , then from Eq.(2) we can obtain the solar wind speed, which is  $598.7\text{ km/s}$ , which fits to the simulated value well.

### 3 OBSERVATIONS

#### 3.1 Instrument setup

The IPS experimental observations were performed from May to December 2008 with the 25 m radio telescope at UAO, China, in SSSF mode. The UAO radio telescope is located to the south of Urumqi city, with 87 deg longitude and 43 deg North latitude. Table 2 shows general information for the 25 m radio telescope receivers currently available at UAO.

The 6 cm and 18 cm bands have dual-polarization cooled receivers, while the 3.6 cm and 13 cm bands have single polarization cooled receivers. Table 3 summarizes some information on the IPS observations we carried out. Compact, strong radio sources selected for observation are listed in table 4.

Test observations were carried out at 49 cm, 18 cm, 13/3.6 cm and 6 cm. Each time the observation was performed on-source for 10 minutes, and off-source for 5 minutes. The integration intervals tried were 1 ms, 5 ms and 10 ms.

According to the characteristics of the IPS phenomenon and synchrotron radiation of radio sources, it would be easier to detect IPS at lower observing frequencies. While the radio environment at UAO

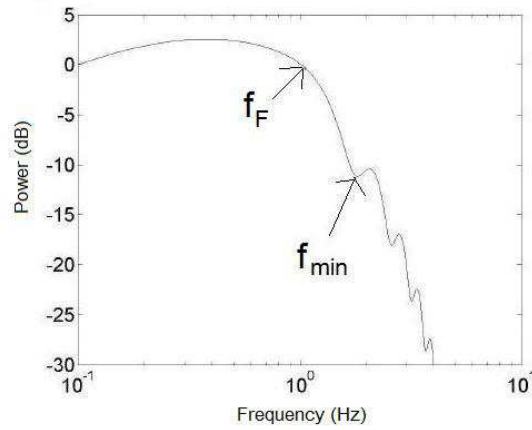


**Fig. 2** Simulation result of SSSF mode,  $\lambda = 92\text{cm}$ ,  $\alpha = 3.5$ ,  $AR = 2.0$ ,  $V = 600\text{km/s}$ ,  $f_F = 1.05\text{Hz}$

Wave length cm	Frequency range MHz	System temperature K	Noise injection K
92	317-337	145	44
30	800-1200	130	40
18	1400-1720	22	3.7
13	2150-2320	75	40
6	4720-5110	21.5	1.7
3.6	8200-8600	40	21
1.3	22100-24000	190	14

**Table 2** Information on the current receivers at UAO, where columns 1-4 give wavelength in cm, frequency range in MHz, system temperature in K, and noise injection in K.

are not good at the 92 cm and 49 cm, so they are seldom used. Consequently we concluded that the 18 cm band is the only window suitable for catching IPS at UAO.

After a series of experiments, the 18 cm dual-polarization receiver at UAO was chosen for the observations, and a data acquisition/receiving system was also established. The data sampling rate is adjustable with 8-bit quantification rate. Being a real-time display system, data quality can be monitored during the observation, so parameters like gain or target source can be adjusted immediately. In order to minimize the RFI (radio frequency interference) influence in the observing window, a band-pass filter was added to the output of IF (intermediate-frequency) of the 18 cm receiver. Figs.3 and 4 show a characteristic spectrum of the 18 cm receiver before and after the filter was added.

Observing wavelength	Dates	Integration interval
cm	mm/dd in 2008	ms
49	5/20-5/23	1/10/20
18	5/20-5/23	1/10/20
	9/25-9/27	0.25
	11/27-12/2	0.25
13	5/20-5/23	1/10/20
6	5/20-5/23	1/10/20
3.6	5/20-5/23	1/10/20

**Table 3** Key parameters of IPS observations with 25 m radio telescope performed in 2008 at UAO, where columns 1-3 give observing wavelength in cm, observing date in mm/dd, and integration interval in ms.

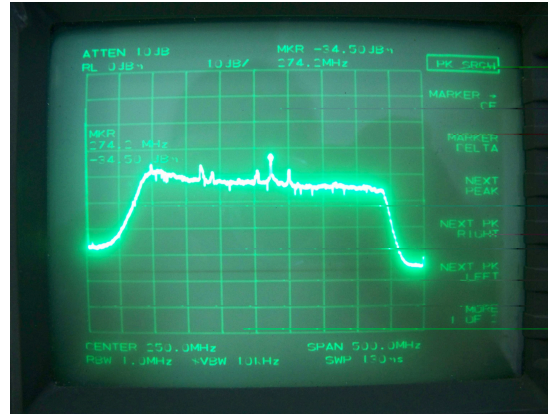
Source	Angular diameter	Flux density (1.4GHz)	Distance from the Sun (Dec. 2008)
	"	Jy	AU
3C345	0.30	7.1	0.3
3C286	0.30	14.9	0.3
3C147	0.15	22.9	0.7

**Table 4** Details of the observed sources, where columns 1-4 give the source name, angular diameter of the source in arc-second, the flux density at 1.4GHz in Jy and the distance from the Sun in AU.

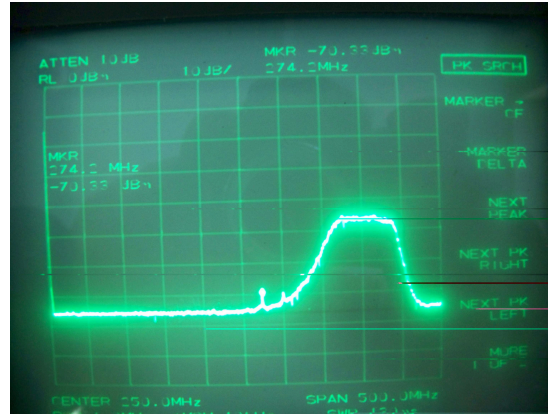
The entire bandwidth at UAO is 500MHz, with some interference in the band as shown in Fig.3. The central frequency of the filter was set to 420MHz, and the 3dB bandwidth was 100MHz, with an insertion loss of 3dB. It can be seen from Fig.4 that the filter works well, the interference in this band has been effectively filtered out. The band selected was the part that with the lowest interference of the whole band. The filter introduces some loss, so we added an amplifier before the radiometer but after the filter.

Fig. 5 is a flowchart of the data acquisition instrument. There is a 0-40 dB step attenuator after the frontend of the 18 cm receiver, with the attenuation step of 1 dB. A PCI8335 high-speed AD image acquisition card was added to our industrial computer, with an input voltage range 0-5V. The AD precision of this card is 16 Bit, with maximum of sampling rate of 250 kHz, and the buffer (FIFO: first in first out) is 8 Kbytes. The radio-meter has two channel outputs. The band of channel A is 5-500 MHz, and the band of channel B is 400-950 MHz. The input power for the two channels is the same: -20 dBm to -60dBm, and the output voltage range of the radiometer is 0-5 V. Channel A was used during





**Fig.3** Characteristic spectrum of 18cm receiver at UAO before filtering



**Fig.4** Characteristic spectrum of 18 cm receiver at UAO after filtering

our observation. Raw data, together with information on the target source like observing time, source coordinates etc., are recorded by the data acquisition software.

During the observations each time the on-source observations were 10 to 15 minutes, and the off-source observations were 5 minutes. In view of the different distances and orientations with respect to the sun, we observed different sources at different times. The total observing time each day was about 2-3 hrs.

### 3.2 Data analysis

In order to eliminate the interference, besides the hardware method (adding a filter), a software solution has also been developed. Figure 6 is the flowchart of the data analysis. First, the raw data observed are played back on the screen to identify the parts with lower noise and one subtracts the noise using software, i.e. the slowly changing component is subtracted from the raw data, and assigned to DATA1. DATA1 is then compared with 3 times the rms error of a long span of data to eliminate wild points. Points with absolute values higher than the 3 rms are omitted and replaced by the average value of the preceding and following data points, then this data is assigned to DATA2. The original integration

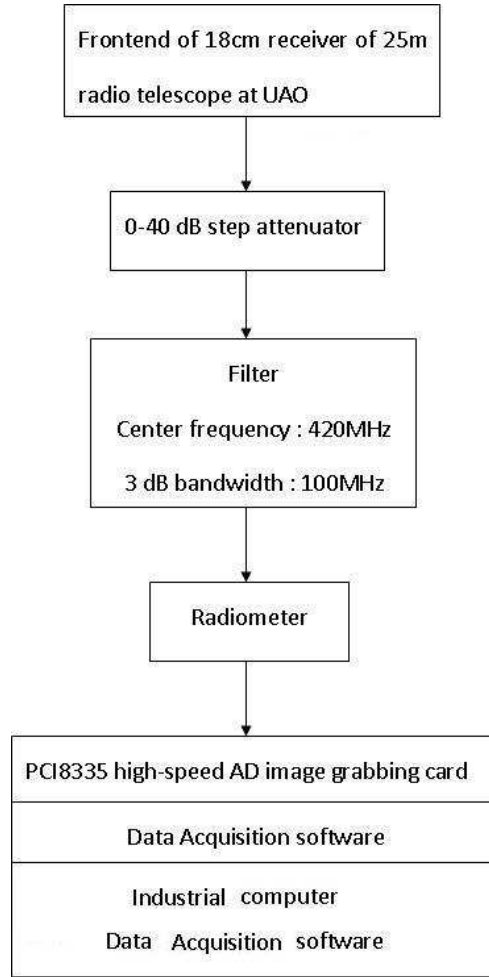


**Fig. 5** Flowchart of data acquisition instrument at UAO for IPS observations

interval of an observation being 0.25 ms, we take the average of four contiguous points to form a 1 ms integration dataset, which means the 10 ms of data are obtained by averaging 40 contiguous points. This data is assigned to DATA3.

In the filtering and re-sampling step, DATA3 is convolved with a rectangular window of suitable width corresponding to the re-sampling rate. The time series is then broken into blocks of length 8192 samples (for 1 ms data approximately 10 s long), and the mean value of each block is subtracted and the block is then multiplied by a triangular weighting function, which is unity at the center and falls to zero at both ends. The result is then transformed by Fourier transformation (FT) to obtain the power spectrum.

### 3.3 Observational results

A series experimental IPS observations were made at UAO. Fig. 7 shows raw data obtained on Nov. 27. The pointed source was 2MASX J18141308-1755351. Its flux density at 1.4 GHz is 5.39 Jy, and its projected distance from sun was 0.23 AU.



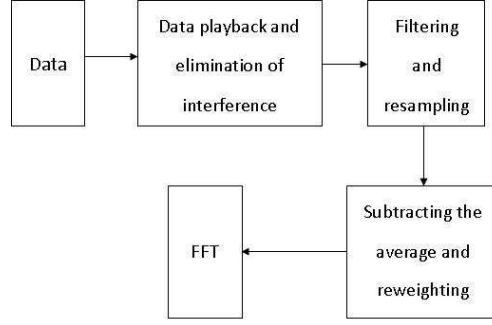


**Fig. 6** Flowchart of data reduction for IPS observations

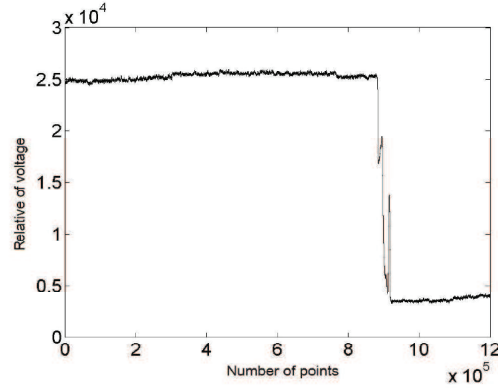


**Fig. 7** Raw dataset display for 2MASX J18141308-1755351, observed on Nov.27, 2008. The  $x$ -axis is the number of points, the  $y$ -axis is the relative of voltage, each point taken with 0.25 ms sampling rate

One can see that the on-source part and off-source part are obviously identified. The fluctuation of the two parts are almost the same, which indicates the IPS phenomenon at the time was weak, which is identical to the power spectrum in Fig. 8. It is clear that the Fresnel knee  $f_F$  and the first minimum frequency  $f_{min}$  are difficult to identify, indicating that there was little scintillation.

Fig. 9 shows a model-fit result of the data taken on Dec. 1, at a wavelength of 18 cm, with an integration interval of 1 ms. The scintillation index is in the range 0.6 to 0.7 (There are some interference in the off source part). The model-fit method is the same as that of SSSF simulation. According to equation (4) to (8), the best parameters can be obtained by fitting with the observing spectra. The target source was 3C345, with a flux density at 1.4 GHz of 7.1 Jy. The solid line shows the observed power spectrum, and the dashed line is the result of parametric model-fitting, with the fitting parameters:  $AR = 1.2$ ,  $\alpha = 3.1$ ,  $V = 400 \text{ km/s}$ . According to OMNI data base, the solar wind speed the whole day ranged between 300 to 400 km/s, which is in agreement with the model-fitted value.

#### 4 CONCLUSIONS

The SSSF mode IPS observations have been studied by quite a number of pioneers (Manoharan et al. 1994). Its instrument, data acquisition, and data reduction are simple. For this mode, high signal-to-

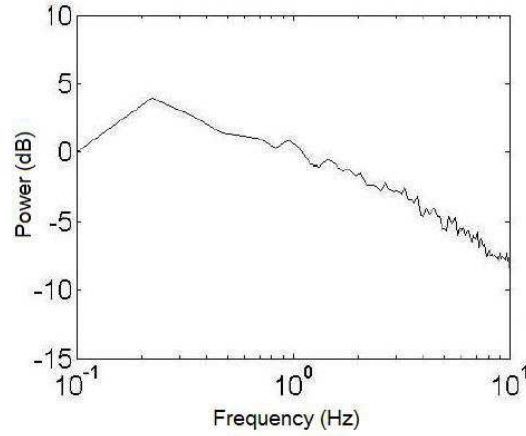


**Fig. 8** Power spectrum result of the target source 2MASX J18141308-1755351 at 18 cm, observed on Nov.27, 2008. The x-axis is power, and the y-axis is frequency

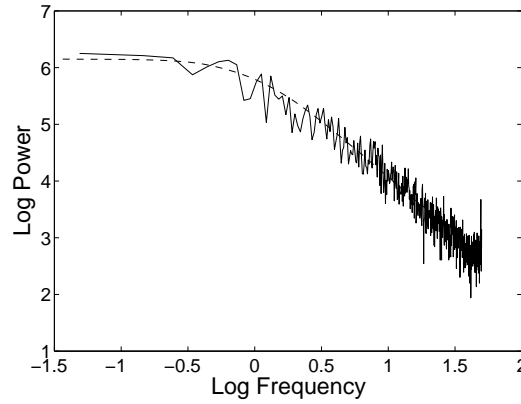


**Fig. 9** Model fitting result on 3C345, observed on Dec.1, 2008 at 18 cm. The solid line shows the observed spectrum of the data, the dashed line is the result of parametric model-fitting.

noise ratio (at least 25dB) data are needed (Tokumaru et al. 1994). When AR increases,  $f_F$  becomes ambiguous, and  $f_{min}$  is easily affected by noise, AR and  $\varepsilon$ . The fitting accuracy is affected by variations in the solar wind parameters, making it hard to calculate the solar wind speed accurately.

Compared with the SSSF mode, the SSDF technique gives the solar wind speed via the first zero point of the cross correlation spectrum, and  $f_{zero}$  is most apparently affected by the velocity of the solar wind rather than other parameters (i.e. Zhang 2007). It has the advantages of higher accuracy on the measurement of solar wind speed and higher stability against the wide variations in solar wind parameters. But it introduces more complexity in the observing instrument and data taking system, it is not used as widely as the SSSF mode.

The new system that is under construction at Miyun station near Beijing, China, with the 50 m radio telescope, adopted the SSDF mode to do the IPS observations. There are some lessons to be learned from the observations with the UAO 25 m radio telescope, such as the integration time of the

receiver system should be sufficiently short since the IPS phenomenon varies rapidly. This implies that the effective receiving area of an IPS antenna should be large enough to ensure that the system has a high instantaneous sensitivity and its band-width should be well-matched to the system time resolution. A bandpass filter and low noise amplifiers (LNA) would be needed to reduce the system noise level.

## 5 ACKNOWLEDGEMENTS

The authors thank all the staff of Urumqi Astronomical Observatory, National Astronomical Observatories, Chinese Academy of Sciences, especially Yi Aili, Yu Aili, N. Wang, X. Liu, H.G. Song, for their help during the observations. We are also grateful to T.Y. Piao and Y.H. Qiu, H.S. Chen, W.J. Han, C.M. Zhang, Y.J. Zheng, for their encouragement and helpful discussions. This work has been supported by the National Meridian Project(grant no.[2006]2176).

## References

- Armstrong J.W., & Coles W.A.:Analysis of three-station interplanetary scintillation.J. Geophys. Res, 77, 4602 - 4610(1972)
- Cohen M. H., Gundermann E. J., Hardebeck H. E.& Sharp L. E.:Interplanetary Scintillations. II Observations. Astrophysical Journal, 147, 449(1967).
- Coles W. A., Harmon J. K.:Interplanetary scintillation measurements of the electron density power spectrum in the solar wind. Journal of Geophysical Research, 83, 1413-1420(1978).
- Coles W.A., Harmon J. K., Lazarus A.J., & Sullivan J.D. :Comparison of 74-MHz interplanetary scintillation and IMP 7 observations of the solar wind during 1973. Journal of Geophysical Research. 83, 3337-3341(1978).
- Hewish A., Scott P.F. & Wills D.:Radio investigation of the solar plasma. Nature, 203, 1214(1964))
- Hewish A., & Symonds M.D.:Radio investigation of the solar plasma. Planetary and Space Science, 17, 313 (1969)
- Kojima M., Asai K., Kozuka Y., Misawa H., Watanabe H.& Yamauchi Y.:Velocity observations at high latitude and the acceleration phenomena. Advances in Space Research, 16, (9)101-(9)110(1995).
- Ma G.Y.:Interplanetary Scintillation Research and Application. Ph D dissertation, BAO(1993).
- Manoharan: Three-dimensional structure of the solar wind: Variation of density with the solar cycle. Solar Physics 148, p153(1993).
- Manoharan P.K., Kojima M.& Misawa H.:The spectrum of electron density fluctuations in the solar wind and its variations with solar wind speed. Journal of Geophysical Research , 99, 23,411-23,420(1994).
- Purvis A., Tappin S. J., Rees W. G., Hewish A.& Duffett-Smith P. J.:The Cambridge IPS survey at 81.5 MHz. Royal Astronomical Society, Monthly Notices, 229, 589-619(1987).
- Scott L., Rickett B.J., & Armstrong J.W.:The velocity and the density spectrum of the solar wind from simultaneous three-frequency IPS observations. Astronomy and Astrophysics, 123, 191-206(1983).
- Swarup G., Sarma N. V. G., Joshi M. N., Kapahi V. K., Bagri D. S., Damle S. V., Ananthakrishnan S., Balasubramanian V., Bhave & Sinha R. P. P.:Large Steerable Radio Telescope at Ootacamund, India. Nature Physical Science, 230, 185(1971).
- Tokumaru M., Mori H., Tanaka T., Kondo T.& Yamauchi Y.:Solar Wind Velocity Near the Sun: Results from Interplanetary Scintillation Observations in 1989-1992. J.Geomag. Geoelectr., 6-10, 401-404(1994).
- Vitkevich V. V., Glushaev A. A., Iliasov Iu. P., Kutuzov S. M., Kuzmin A. D., Alekseev I. A., Bunin V. D., Novozhenov G. F., Pavlov G. A.& Solomin N. S.:Antenna equipment of the Lebedev Institute BSA radio telescope facility. Radiofizika, 19, 1594-1606(1976).
- Walker, M. A., Melrose D.B., Stinbring, D.R. & Zhang, C.M.: Interpretation of parabolic arcs in pulsar secondary spectra. MNRAS, 354, 43-54 (2004).
- Wang S.G.: Some Suggestion for IPS Observations in MSRT. Personal letter(1990).
- Wu J.H., Zhang X.Z., & Zheng Y.J. Ap&SS, 278, 189(2001).
- Ye P.Z., Qiu Y.H.:Single Station Interplanetary Scintillation Measurement to Diagnose Solar Wind Velocity. Acta Astrophysica Sinica, 16, 389-394(1996).

Zhang X.Z.: A Study on the Technique of Observing Interplanetary Scintillation with Simultaneous Dual-frequency Measurement. *Chin. J. Astron. & Astrophys.* 7, 5, 712-720 (2007).

Zhang X. Z., Wu J. H.: IPS Observations at Miyun Station, BAO. *Astronomical Society of the Pacific*, 1-58381-069-2, 2001, 580 (2001)

## Observation of Interplanetary Scintillation with Single-Station Mode at Urumqi

Lijia Liu<sup>1</sup>, Xizhen Zhang<sup>1</sup>, Jianbin Li<sup>1</sup>, P.K. Manoharan<sup>2</sup>, Zhiyong Liu<sup>3</sup> and Bo Peng<sup>1</sup>

<sup>1</sup> National Astronomical Observatories, Chinese Academy of Sciences, Beijing 100012, China; [liulijia@redstar@yahoo.com.cn](mailto:liulijia@redstar@yahoo.com.cn), [lijb@bao.ac.cn](mailto:lijb@bao.ac.cn), [zxz@bao.ac.cn](mailto:zxz@bao.ac.cn), [pb@bao.ac.cn](mailto:pb@bao.ac.cn)

<sup>2</sup> Radio Astronomy Center, TIFR-NCRA, P.O. Box 8, Ooty 643 001, India; [mano@ncra.tifr.res.in](mailto:mano@ncra.tifr.res.in)

<sup>3</sup> Urumqi Observatory, NAOC No.150 South Science Road Urumqi, Xinjiang 830011, China; [liuzhy@uao.ac.cn](mailto:liuzhy@uao.ac.cn)

**Abstract** The Sun affects the Earth's physical phenomena in multiple ways, in particular the material in interplanetary space comes from coronal expansion in the form of inhomogeneous plasma flow (solar wind), which is the primary source of the interplanetary medium. Ground-based Interplanetary Scintillation (IPS) observations are an important and effective method for measuring solar wind speed and the structures of small diameter radio sources. We discuss one mode of ground-based single-station observations: Single-Station Single-Frequency (SSSF) mode. To realize the SSSF mode, a new system has been established at Urumqi Astronomical Observatory (UAO), China, and a series of experimental observations were carried out successfully from May to December, 2008.

**Key words:** IPS-SSSF-Observation

### 1 INTRODUCTION

Radiation from a distant compact radio source is scattered by the density irregularities in the solar wind plasma and produces a random diffraction pattern on the ground. The motion of these irregularities converts this pattern into temporal intensity fluctuations which are observed as interplanetary scintillation (IPS). IPS observations with ground-based telescopes can estimate the solar wind velocity and also the structures of the distant compact radio sources (Hewish & Symonds 1969; Armstrong & Coles 1972). This kind of measurement, though indirect, can give information on the solar wind out of the ecliptic plane and close to the Sun, where direct spacecraft measurements are not possible (e.g. Ma 1993). Here we concentrate on extracting information on solar wind speed from IPS observations with ground-based single telescope.

There are two modes to observe the IPS phenomenon with a single-station: Single-Station Single-Frequency (SSSF) and Single-Station Dual-Frequency (SSDF). Since the discovery of the IPS phenomenon (Hewish et al. 1964), many countries began doing IPS observations with the single-station method, i.e. Cambridge telescope in Britain (Pruvis et al. 1987), Ooty radio telescope in India (Swarup et al. 1971), Puschino observatory in Russia (Vitkevich et al. 1976), one can use the power spectral fitting method to obtain the solar wind speed. With the multi-station method as used in Japan, which is a three-station system (Kojima et al. 1995), one can measure the projected solar wind speed directly. China began IPS studies from the 1990s with the phased array mode of the Miyun Synthesis Radio Telescope (MSRT) at 232 MHz. Located at Miyun observatory (Wang 1990) in Beijing, it used the SSSF mode (Wu & Zhang 2001). Recently a new IPS observation system using the 50 m parabolic radio telescope,

which is based on the SSDF mode at S/X and UHF bands, is under construction to serve the National Meridian Project of China.

In this paper, the theory of IPS, the technique, and the numerical simulation method of SSSF mode are introduced in section 2. The observations carried out at the UAO are reported in section 3. Finally conclusions are drawn in Section 4.

## 2 THEORY

### 2.1 The Theory of IPS

Interplanetary scintillation is the name given to the intensity fluctuations of small diameter radio sources which are caused by density inhomogeneities in the solar wind. Figure 1 shows the geometry of IPS. The distance between the Sun and  $Q$  is  $r$ , and  $r = \sin(\varepsilon)AU$ .

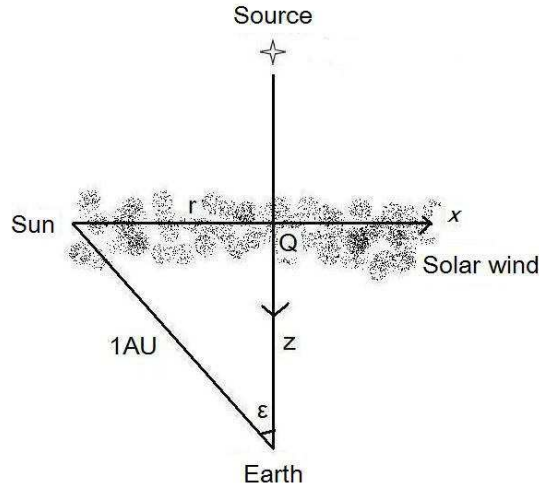


**Fig. 1** IPS Geometry:  $z$ -axis is along the line-of-sight,  $x$ -axis is in the direction perpendicular to the  $z$ -axis pointing away from the Sun, and  $y$ -axis is normal to the paper.  $Q$  is the point closest to the Sun along the line-of-sight, and  $\varepsilon$  is the elongation angle, Sun-Earth-source.  $r$  is the distance between the Sun and  $Q$ .  $Z$  is the distance between  $Q$  and the Earth.

The degree of scintillation is characterized by the scintillation index  $m$  (Cohen et al. 1967), which increases with decreasing distance  $r$  until it reaches a maximum  $m_{max}$  at  $r_{min}$ .  $r_{min}$  changes with frequency,  $r_{min} \approx 0.2AU$  for meter wavelength (Manoharan, 1993).

$$m = \frac{\sqrt{\sigma_{on}^2 - \sigma_{off}^2}}{C_{on} - C_{off}} \quad (1)$$

where  $C_{on}$  ( $C_{off}$ ) is the average intensity of the on-source (off-source) signal, and  $\sigma_{on}^2$  ( $\sigma_{off}^2$ ) is the square of rms of intensity scintillation. Here on-source case refers the telescope pointing at the radio source, and off-source the telescope pointing at the background sky away from the source, being in the opposite pitching direction to where the radio source moves. IPS is strongest in the region nearest the Sun, where we have the "strong scintillation region". In most of interplanetary space IPS is weak, which is called the "weak scintillation region" (Zhang 2006). In the weak scintillation region,  $m^2 \ll 1$ . The weak scintillation region is observed at  $r > r_{min}$  and strong scintillation is observed at  $r < r_{min}$ . Previous studies show that the statistics of the scintillation are simply related to those of the turbulent

interplanetary medium by a linear relationship, if the scintillation is weak (Coles & Harmon 1978). In the "strong scintillation region", however, the relationship is not straight forward, and the present study always deals with the weak scintillation case. The distance regime for the weak and strong regions relates to observing frequencies. Table 1 shows the relationship between the frequency and distance regimes (Zhang 2006).

Frequency (MHz)	150	327	900	2000	5000
Heliocentric distance (solar radius)	60	35	18	10	5

**Table 1** Regions of strong and weak scintillation at different frequencies. Taking 327 MHz for example, the regimes for the strong and weak regions are within 35 solar radius and beyond respectively.

In the weak scintillation region, where the radio wave can be treated as a plane-wave, and the Born approximation is applicable (e.g. Walker et al. 2004), the interplanetary medium can be considered to be made up of many thin layers perpendicular to the line-of-sight. When the radio wave passes through these layers, only the phase of the radio wave changes, while the amplitude of the radio wave stays the same. This is called the "thin screen approximation", which is commonly used in the study of the ionosphere, interplanetary medium, and interstellar medium.

## 2.2 SSSF Mode

SSSF refers to observing the IPS with a single station at a single frequency. There are two methods to obtain the solar wind speed from SSSF mode observed spectra: the spectral multi-parameter model-fitting, and the characteristic frequencies methods. The former can measure the speed by adjusting the main parameters of the solar wind to fit the observed scintillation power spectra. The parameters are:  $\alpha$ -power law index of the spatial spectrum of electron density, AR-axial ratio of solar wind irregularities, and  $V$ -solar wind speed. The latter can be determined by calculating two characteristic frequencies of the spectra: the Fresnel knee frequency  $f_F$ , and  $f_{min}$  the first minimum of the spectra. Then the solar wind speed can be calculated by either of the formulas shown below (Scott et al. 1983)

$$V = f_F \sqrt{Z\pi\lambda} \quad (2)$$

$$V = f_{min} \sqrt{Z\lambda} \quad (3)$$

where  $\lambda$  is the observing wavelength,  $Z$  is the distance between  $Q$  and the Earth as shown in Fig. 1. According to weak scintillation theory and thin screen approximation theory, in the weak scintillation region, the observed scintillation can be regarded as the sum of contributions from all the thin layers. For a layer of thickness  $dZ$ , the distance from the layer to the Earth is  $Z$ ,  $V_x(z)$  is the solar wind velocity projected on to the plane perpendicular to the direction  $z$ , and the spectra observed at the Earth should be (e.g. Scott et al. 1983; Ye & Qiu 1996):

$$M_s(f, Z)dZ = \frac{2\pi f(\lambda r_e)^2}{V_x(z)} \int_{-\infty}^{\infty} \Phi_{ne}(k_x, k_y, k_z = 0, Z) \times F_d F_s dk_y dZ \quad (4)$$



where,

$$F_d = 4 \sin^2 \left[ \frac{(k_x^2 + k_y^2) \lambda Z}{4\pi} \right] \quad (5)$$

$$F_s = \exp[-(k_x^2 + k_y^2) Z^2 \theta_0^2] \quad (6)$$

Here  $F_d$  and  $F_s$  are the Fresnel propagation filter parameter and the squared modulus of the radio source visibility. We assume that the brightness of the radio source has a symmetrical-Gaussian distribution, i.e.  $B(\theta) = \exp[\frac{-(\theta/\theta_0)^2}{2}]$ .  $\Theta$  is the full width at half maximum of the source, so we have the angular diameter of the scintillating source  $\theta_0 = \Theta/2.35$  (Manoharan & Ananthakrishnan 1990).  $\Phi_{ne}$  is the electron density power spectrum at distance  $z$ ,

$$\Phi_{ne}(k_x, k_y, k_z = 0, Z) = T r^{-4} [k_x^2 + (k_y/AR)^2]^{-\alpha/2} \quad (7)$$

where the amplitude of fluctuations in the electron density  $T$  is a constant. The spectrum obtained from the Earth should be the sum of Eq. (4).

$$M_i(f) = \int_0^\infty M_s(f, Z) dZ \quad (8)$$

One can see that  $M_i(f)$  depends on the solar wind parameters: axis ratio  $AR$ , power law index  $\alpha$ , and the solar wind speed  $V$ . Previous studies show that, when other parameters fixed,  $AR$  mostly affects the low frequency part of the power spectra; when  $AR$  increases, the low frequency part becomes steeper, but the high frequency part changes slightly.  $\alpha$  mostly affects the high frequency part of the spectra; when  $\alpha$  increases, the high frequency part attenuates quickly, but the low frequency part changes invidently. The solar wind speed  $V$  mostly affects the Fresnel knee  $f_F$  and the first minimum of the spectra  $f_{min}$ ; the two frequencies both become larger when  $V$  increases. Taking appropriate values to fit the observed spectra, one can obtain the parameters of the observational data. Firstly one fits the fresnel knee according to  $f_F$  and  $f_{min}$ , then fits the attenuated high part and the flat low frequency part. (Ye & Qiu 1996)

Fig.2 is an example of the SSSF mode. Where the parameters taken are  $\lambda = 92\text{cm}$ ,  $\alpha = 3.5$ ,  $AR = 2.0$ ,  $V = 600\text{km/s}$ ,  $\theta_0 = 0.02''$ . One can get  $f_F = 1.05\text{Hz}$ , then from Eq.(2) we can obtain the solar wind speed, which is  $598.7\text{ km/s}$ , which fits to the simulated value well.

### 3 OBSERVATIONS

#### 3.1 Instrument setup

The IPS experimental observations were performed from May to December 2008 with the 25 m radio telescope at UAO, China, in SSSF mode. The UAO radio telescope is located to the south of Urumqi city, with 87 deg longitude and 43 deg North latitude. Table 2 shows general information for the 25 m radio telescope receivers currently available at UAO.

The 6 cm and 18 cm bands have dual-polarization cooled receivers, while the 3.6 cm and 13 cm bands have single polarization cooled receivers. Table 3 summarizes some information on the IPS observations we carried out. Compact, strong radio sources selected for observation are listed in table 4.

Test observations were carried out at 49 cm, 18 cm, 13/3.6 cm and 6 cm. Each time the observation was performed on-source for 10 minutes, and off-source for 5 minutes. The integration intervals tried were 1 ms, 5 ms and 10 ms.

According to the characteristics of the IPS phenomenon and synchrotron radiation of radio sources, it would be easier to detect IPS at lower observing frequencies. While the radio environment at UAO

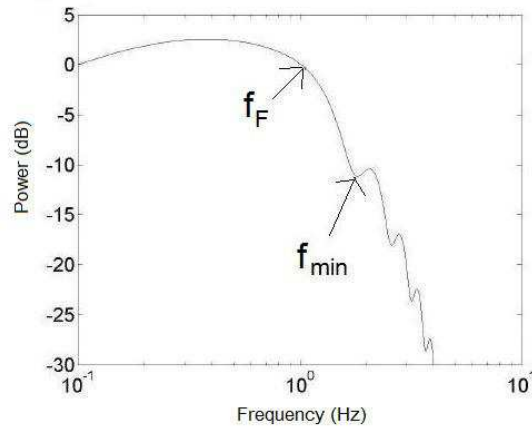


**Fig. 2** Simulation result of SSSF mode,  $\lambda = 92\text{cm}$ ,  $\alpha = 3.5$ ,  $AR = 2.0$ ,  $V = 600\text{km/s}$ ,  $f_F = 1.05\text{Hz}$

Wave length cm	Frequency range MHz	System temperature K	Noise injection K
92	317-337	145	44
30	800-1200	130	40
18	1400-1720	22	3.7
13	2150-2320	75	40
6	4720-5110	21.5	1.7
3.6	8200-8600	40	21
1.3	22100-24000	190	14

**Table 2** Information on the current receivers at UAO, where columns 1-4 give wavelength in cm, frequency range in MHz, system temperature in K, and noise injection in K.

are not good at the 92 cm and 49 cm, so they are seldom used. Consequently we concluded that the 18 cm band is the only window suitable for catching IPS at UAO.

After a series of experiments, the 18 cm dual-polarization receiver at UAO was chosen for the observations, and a data acquisition/receiving system was also established. The data sampling rate is adjustable with 8-bit quantification rate. Being a real-time display system, data quality can be monitored during the observation, so parameters like gain or target source can be adjusted immediately. In order to minimize the RFI (radio frequency interference) influence in the observing window, a band-pass filter was added to the output of IF (intermediate-frequency) of the 18 cm receiver. Figs.3 and 4 show a characteristic spectrum of the 18 cm receiver before and after the filter was added.

Observing wavelength	Dates	Integration interval
cm	mm/dd in 2008	ms
49	5/20-5/23	1/10/20
18	5/20-5/23	1/10/20
	9/25-9/27	0.25
	11/27-12/2	0.25
13	5/20-5/23	1/10/20
6	5/20-5/23	1/10/20
3.6	5/20-5/23	1/10/20

**Table 3** Key parameters of IPS observations with 25 m radio telescope performed in 2008 at UAO, where columns 1-3 give observing wavelength in cm, observing date in mm/dd, and integration interval in ms.

Source	Angular diameter	Flux density (1.4GHz)	Distance from the Sun (Dec. 2008)
	"	Jy	AU
3C345	0.30	7.1	0.3
3C286	0.30	14.9	0.3
3C147	0.15	22.9	0.7

**Table 4** Details of the observed sources, where columns 1-4 give the source name, angular diameter of the source in arc-second, the flux density at 1.4GHz in Jy and the distance from the Sun in AU.

The entire bandwidth at UAO is 500MHz, with some interference in the band as shown in Fig.3. The central frequency of the filter was set to 420MHz, and the 3dB bandwidth was 100MHz, with an insertion loss of 3dB. It can be seen from Fig.4 that the filter works well, the interference in this band has been effectively filtered out. The band selected was the part that with the lowest interference of the whole band. The filter introduces some loss, so we added an amplifier before the radiometer but after the filter.

Fig. 5 is a flowchart of the data acquisition instrument. There is a 0-40 dB step attenuator after the frontend of the 18 cm receiver, with the attenuation step of 1 dB. A PCI8335 high-speed AD image acquisition card was added to our industrial computer, with an input voltage range 0-5V. The AD precision of this card is 16 Bit, with maximum of sampling rate of 250 kHz, and the buffer (FIFO: first in first out) is 8 Kbytes. The radio-meter has two channel outputs. The band of channel A is 5-500 MHz, and the band of channel B is 400-950 MHz. The input power for the two channels is the same: -20 dBm to -60dBm, and the output voltage range of the radiometer is 0-5 V. Channel A was used during

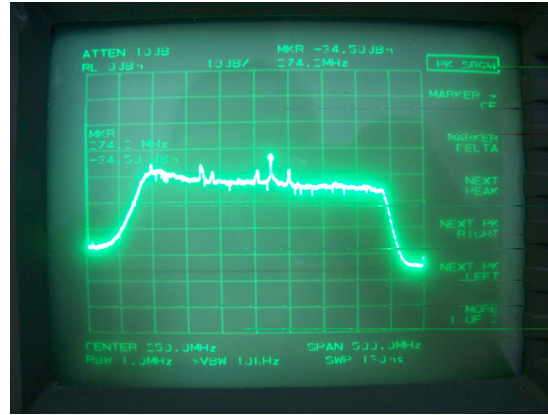


**Fig.3** Characteristic spectrum of 18cm receiver at UAO before filtering

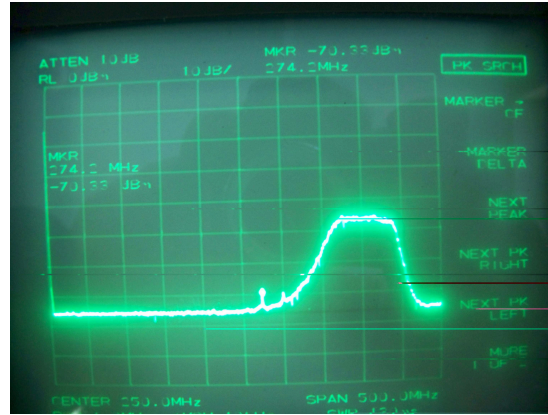


**Fig.4** Characteristic spectrum of 18 cm receiver at UAO after filtering

our observation. Raw data, together with information on the target source like observing time, source coordinates etc., are recorded by the data acquisition software.

During the observations each time the on-source observations were 10 to 15 minutes, and the off-source observations were 5 minutes. In view of the different distances and orientations with respect to the sun, we observed different sources at different times. The total observing time each day was about 2-3 hrs.

### 3.2 Data analysis

In order to eliminate the interference, besides the hardware method (adding a filter), a software solution has also been developed. Figure 6 is the flowchart of the data analysis. First, the raw data observed are played back on the screen to identify the parts with lower noise and one subtracts the noise using software, i.e. the slowly changing component is subtracted from the raw data, and assigned to DATA1. DATA1 is then compared with 3 times the rms error of a long span of data to eliminate wild points. Points with absolute values higher than the 3 rms are omitted and replaced by the average value of the preceding and following data points, then this data is assigned to DATA2. The original integration

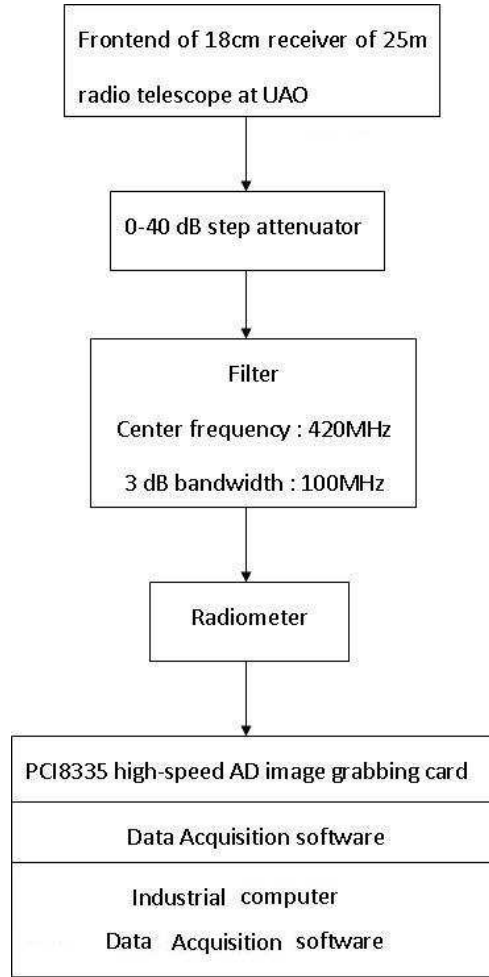


**Fig. 5** Flowchart of data acquisition instrument at UAO for IPS observations

interval of an observation being 0.25 ms, we take the average of four contiguous points to form a 1 ms integration dataset, which means the 10 ms of data are obtained by averaging 40 contiguous points. This data is assigned to DATA3.

In the filtering and re-sampling step, DATA3 is convolved with a rectangular window of suitable width corresponding to the re-sampling rate. The time series is then broken into blocks of length 8192 samples (for 1 ms data approximately 10 s long), and the mean value of each block is subtracted and the block is then multiplied by a triangular weighting function, which is unity at the center and falls to zero at both ends. The result is then transformed by Fourier transformation (FT) to obtain the power spectrum.

### 3.3 Observational results

A series experimental IPS observations were made at UAO. Fig. 7 shows raw data obtained on Nov. 27. The pointed source was 2MASX J18141308-1755351. Its flux density at 1.4 GHz is 5.39 Jy, and its projected distance from sun was 0.23 AU.

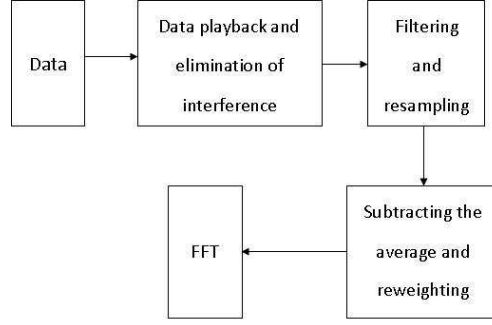


**Fig. 6** Flowchart of data reduction for IPS observations

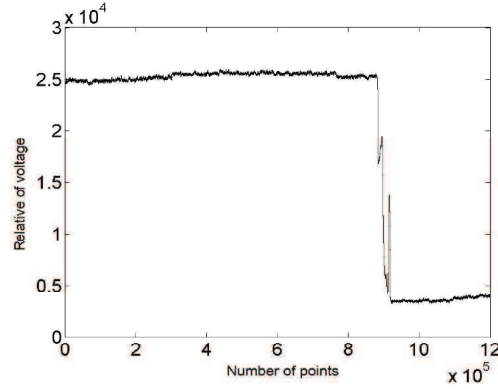


**Fig. 7** Raw dataset display for 2MASX J18141308-1755351, observed on Nov.27, 2008. The  $x$ -axis is the number of points, the  $y$ -axis is the relative of voltage, each point taken with 0.25 ms sampling rate

One can see that the on-source part and off-source part are obviously identified. The fluctuation of the two parts are almost the same, which indicates the IPS phenomenon at the time was weak, which is identical to the power spectrum in Fig. 8. It is clear that the Fresnel knee  $f_F$  and the first minimum frequency  $f_{min}$  are difficult to identify, indicating that there was little scintillation.

Fig. 9 shows a model-fit result of the data taken on Dec. 1, at a wavelength of 18 cm, with an integration interval of 1 ms. The scintillation index is in the range 0.6 to 0.7 (There are some interference in the off source part). The model-fit method is the same as that of SSSF simulation. According to equation (4) to (8), the best parameters can be obtained by fitting with the observing spectra. The target source was 3C345, with a flux density at 1.4 GHz of 7.1 Jy. The solid line shows the observed power spectrum, and the dashed line is the result of parametric model-fitting, with the fitting parameters:  $AR = 1.2$ ,  $\alpha = 3.1$ ,  $V = 400 \text{ km/s}$ . According to OMNI data base, the solar wind speed the whole day ranged between 300 to 400 km/s, which is in agreement with the model-fitted value.

#### 4 CONCLUSIONS

The SSSF mode IPS observations have been studied by quite a number of pioneers (Manoharan et al. 1994). Its instrument, data acquisition, and data reduction are simple. For this mode, high signal-to-

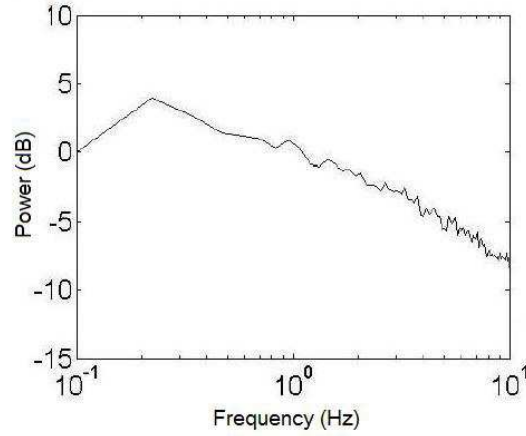


**Fig. 8** Power spectrum result of the target source 2MASX J18141308-1755351 at 18 cm, observed on Nov.27, 2008. The x-axis is power, and the y-axis is frequency

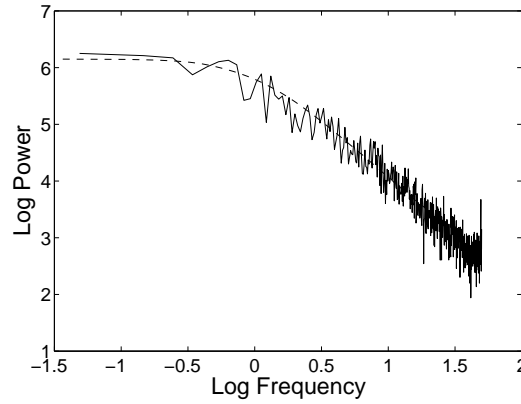


**Fig. 9** Model fitting result on 3C345, observed on Dec.1, 2008 at 18 cm. The solid line shows the observed spectrum of the data, the dashed line is the result of parametric model-fitting.

noise ratio (at least 25dB) data are needed (Tokumaru et al. 1994). When AR increases,  $f_F$  becomes ambiguous, and  $f_{min}$  is easily affected by noise, AR and  $\varepsilon$ . The fitting accuracy is affected by variations in the solar wind parameters, making it hard to calculate the solar wind speed accurately.

Compared with the SSSF mode, the SSDF technique gives the solar wind speed via the first zero point of the cross correlation spectrum, and  $f_{zero}$  is most apparently affected by the velocity of the solar wind rather than other parameters (i.e. Zhang 2007). It has the advantages of higher accuracy on the measurement of solar wind speed and higher stability against the wide variations in solar wind parameters. But it introduces more complexity in the observing instrument and data taking system, it is not used as widely as the SSSF mode.

The new system that is under construction at Miyun station near Beijing, China, with the 50 m radio telescope, adopted the SSDF mode to do the IPS observations. There are some lessons to be learned from the observations with the UAO 25 m radio telescope, such as the integration time of the



receiver system should be sufficiently short since the IPS phenomenon varies rapidly. This implies that the effective receiving area of an IPS antenna should be large enough to ensure that the system has a high instantaneous sensitivity and its band-width should be well-matched to the system time resolution. A bandpass filter and low noise amplifiers (LNA) would be needed to reduce the system noise level.

## 5 ACKNOWLEDGEMENTS

The authors thank all the staff of Urumqi Astronomical Observatory, National Astronomical Observatories, Chinese Academy of Sciences, especially Yi Aili, Yu Aili, N. Wang, X. Liu, H.G. Song, for their help during the observations. We are also grateful to T.Y. Piao and Y.H. Qiu, H.S. Chen, W.J. Han, C.M. Zhang, Y.J. Zheng, for their encouragement and helpful discussions. This work has been supported by the National Meridian Project(grant no.[2006]2176).

## References

- Armstrong J.W., & Coles W.A.:Analysis of three-station interplanetary scintillation.J. Geophys. Res, 77, 4602 - 4610(1972)
- Cohen M. H., Gundermann E. J., Hardebeck H. E.& Sharp L. E.:Interplanetary Scintillations. II Observations. Astrophysical Journal, 147, 449(1967).
- Coles W. A., Harmon J. K.:Interplanetary scintillation measurements of the electron density power spectrum in the solar wind. Journal of Geophysical Research, 83, 1413-1420(1978).
- Coles W.A., Harmon J. K., Lazarus A.J., & Sullivan J.D. :Comparison of 74-MHz interplanetary scintillation and IMP 7 observations of the solar wind during 1973. Journal of Geophysical Research. 83, 3337-3341(1978).
- Hewish A., Scott P.F. & Wills D.:Radio investigation of the solar plasma. Nature, 203, 1214(1964))
- Hewish A., & Symonds M.D.:Radio investigation of the solar plasma. Planetary and Space Science, 17, 313 (1969)
- Kojima M., Asai K., Kozuka Y., Misawa H., Watanabe H.& Yamauchi Y.:Velocity observations at high latitude and the acceleration phenomena. Advances in Space Research, 16, (9)101-(9)110(1995).
- Ma G.Y.:Interplanetary Scintillation Research and Application. Ph D dissertation, BAO(1993).
- Manoharan: Three-dimensional structure of the solar wind: Variation of density with the solar cycle. Solar Physics 148, p153(1993).
- Manoharan P.K., Kojima M.& Misawa H.:The spectrum of electron density fluctuations in the solar wind and its variations with solar wind speed. Journal of Geophysical Research , 99, 23,411-23,420(1994).
- Purvis A., Tappin S. J., Rees W. G., Hewish A.& Duffett-Smith P. J.:The Cambridge IPS survey at 81.5 MHz. Royal Astronomical Society, Monthly Notices, 229, 589-619(1987).
- Scott L., Rickett B.J., & Armstrong J.W.:The velocity and the density spectrum of the solar wind from simultaneous three-frequency IPS observations. Astronomy and Astrophysics, 123, 191-206(1983).
- Swarup G., Sarma N. V. G., Joshi M. N., Kapahi V. K., Bagri D. S., Damle S. V., Ananthakrishnan S., Balasubramanian V., Bhave & Sinha R. P. P.:Large Steerable Radio Telescope at Ootacamund, India. Nature Physical Science, 230, 185(1971).
- Tokumaru M., Mori H., Tanaka T., Kondo T.& Yamauchi Y.:Solar Wind Velocity Near the Sun: Results from Interplanetary Scintillation Observations in 1989-1992. J.Geomag. Geoelectr., 6-10, 401-404(1994).
- Vitkevich V. V., Glushaev A. A., Iliasov Iu. P., Kutuzov S. M., Kuzmin A. D., Alekseev I. A., Bunin V. D., Novozhenov G. F., Pavlov G. A.& Solomin N. S.:Antenna equipment of the Lebedev Institute BSA radio telescope facility. Radiofizika, 19, 1594-1606(1976).
- Walker, M. A., Melrose D.B., Stinbring, D.R. & Zhang, C.M.: Interpretation of parabolic arcs in pulsar secondary spectra. MNRAS, 354, 43-54 (2004).
- Wang S.G.: Some Suggestion for IPS Observations in MSRT. Personal letter(1990).
- Wu J.H., Zhang X.Z., & Zheng Y.J. Ap&SS, 278, 189(2001).
- Ye P.Z., Qiu Y.H.:Single Station Interplanetary Scintillation Measurement to Diagnose Solar Wind Velocity. Acta Astrophysica Sinica, 16, 389-394(1996).

Zhang X.Z.: A Study on the Technique of Observing Interplanetary Scintillation with Simultaneous Dual-frequency Measurement. *Chin. J. Astron. & Astrophys.* 7, 5, 712-720 (2007).

Zhang X. Z., Wu J. H.: IPS Observations at Miyun Station, BAO. *Astronomical Society of the Pacific*, 1-58381-069-2, 2001, 580 (2001)